



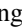





Nodeless kagome superconductivity in  $\text{LaRu}_3\text{Si}_2$ 

C. Mielke, III <sup>1,2,\*</sup>, Y. Qin,<sup>3,\*</sup> J.-X. Yin,<sup>4,\*</sup> H. Nakamura,<sup>5,\*</sup> D. Das <sup>1</sup>, K. Guo <sup>6,7</sup>, R. Khasanov <sup>1</sup>, J. Chang <sup>2</sup>, Z. Q. Wang,<sup>8</sup> S. Jia,<sup>6,7</sup> S. Nakatsuji,<sup>5</sup> A. Amato <sup>1</sup>, H. Luetkens <sup>1</sup>, G. Xu,<sup>3,†</sup> M. Z. Hasan,<sup>4,9,10,11,‡</sup> and Z. Guguchia <sup>1,§</sup>

<sup>1</sup>Laboratory for Muon Spin Spectroscopy, Paul Scherrer Institute, CH-5232 Villigen PSI, Switzerland

<sup>2</sup>Physik-Institut, Universität Zurich, Winterthurerstrasse 190, CH-8057 Zurich, Switzerland

<sup>3</sup>Wuhan National High Magnetic Field Center and School of Physics, Huazhong University of Science and Technology, Wuhan 430074, China

<sup>4</sup>Laboratory for Topological Quantum Matter and Advanced Spectroscopy (B7), Department of Physics, Princeton University, Princeton, New Jersey 08544, USA

<sup>5</sup>Institute for Solid State Physics, University of Tokyo, Kashiwa, 277-8581, Japan

<sup>6</sup>International Center for Quantum Materials and School of Physics, Peking University, Beijing 100871, China

<sup>7</sup>CAS Center for Excellence in Topological Quantum Computation, University of Chinese Academy of Science, Beijing 100864, China

<sup>8</sup>Department of Physics, Boston College, Chestnut Hill, Massachusetts 02467, USA

<sup>9</sup>Princeton Institute for the Science and Technology of Materials, Princeton University, Princeton, New Jersey 08540, USA

<sup>10</sup>Materials Sciences Division, Lawrence Berkeley National Laboratory, Berkeley, California 94720, USA

<sup>11</sup>Quantum Science Center, Oak Ridge, Tennessee 37831, USA



(Received 1 January 2021; revised 15 February 2021; accepted 8 March 2021; published 29 March 2021)

We report muon spin rotation ( $\mu\text{SR}$ ) experiments together with first-principles calculations on microscopic properties of superconductivity in the kagome superconductor  $\text{LaRu}_3\text{Si}_2$  with  $T_c \simeq 7\text{K}$ . Below  $T_c$ ,  $\mu\text{SR}$  reveals type-II superconductivity with a single  $s$ -wave gap, which is robust against hydrostatic pressure up to 2 GPa. We find that the calculated normal state band structure features a kagome flat band, and Dirac as well as van Hove points formed by the  $\text{Ru-}d_{z^2}$  orbitals near the Fermi level. We also find that electron-phonon coupling alone can only reproduce a small fraction of  $T_c$  from calculations, which suggests other factors in enhancing  $T_c$  such as the correlation effect from the kagome flat band, the van Hove point on the kagome lattice, and the high density of states from narrow kagome bands. Our experiments and calculations taken together point to nodeless moderate coupling kagome superconductivity in  $\text{LaRu}_3\text{Si}_2$ .

DOI: [10.1103/PhysRevMaterials.5.034803](https://doi.org/10.1103/PhysRevMaterials.5.034803)

## I. INTRODUCTION

Layered systems with highly anisotropic electronic properties have been found to be potential hosts for rich, unconventional, and exotic quantum states. The prominent class of layered materials are the kagome-lattice systems [1–7]. Crystalline materials that contain a kagome lattice have attracted considerable attention because of the associated electronic band structure and frustrated antiferromagnetic (AFM) interactions. This band structure reveals a pair of Dirac points similar to those found in graphene, and a dispersionless, flat band that originates from the kinetic frustration associated with the geometry of the kagome lattice. Flat bands are exciting because the associated high density of electronic states hints at possible correlated electronic phases when found close to the Fermi level [8–10]. The possibility of accessing flat bands and their influence on the physical properties of the system has been studied for about three decades [10–17]. Recently, superconductivity was discovered in bilayer graphene [18] when its individual layers are twisted with respect to each other by a specific angle, giving rise to a flat band. Recent

Monte Carlo calculations on a two-dimensional system [8] demonstrate that the ground state is a superconductor and find a broad pseudogap regime that exhibits strong pairing fluctuations and even a tendency towards electronic phase separation. Moreover, a square-octagon lattice was theoretically studied. Two perfectly flat bands were found [9] and the calculated superconducting phase diagram was found to have two superconducting domes [9], as observed in several types of unconventional superconductors. Thus, there is a resurgence of interest from the experimental front in flat bands as a means to explore unconventional superconductivity [8,19,20].

In this framework, the layered system  $\text{LaRu}_3\text{Si}_2$  [21–25] appears to be a good example of a material hosting both a kagome lattice and superconductivity. The structure of  $\text{LaRu}_3\text{Si}_2$  contains distorted kagome layers of Ru sandwiched between layers of La and layers of Si having a honeycomb structure [see Figs. 1(a) and 1(b)], crystallizing in the  $P6_3/m$  space group. The system was shown to be a typical type II superconductor with a superconductivity (SC) transition temperature with the onset as high as  $\simeq 7\text{K}$  [23]. Anomalous properties [25] in the normal and SC states [23] were reported in  $\text{LaRu}_3\text{Si}_2$ , such as the deviation of the normal state specific heat from the Debye model, nonmean field-like suppression of superconductivity with magnetic field, and nonlinear field dependence of the induced quasiparticle density of states (DOS). However, for the most part only the critical temperatures and fields have been characterized for the superconducting state

\*These authors contributed equally to the paper.

†gangxu@hust.edu.cn

‡mzhasan@princeton.edu

§zurab.guguchia@psi.ch

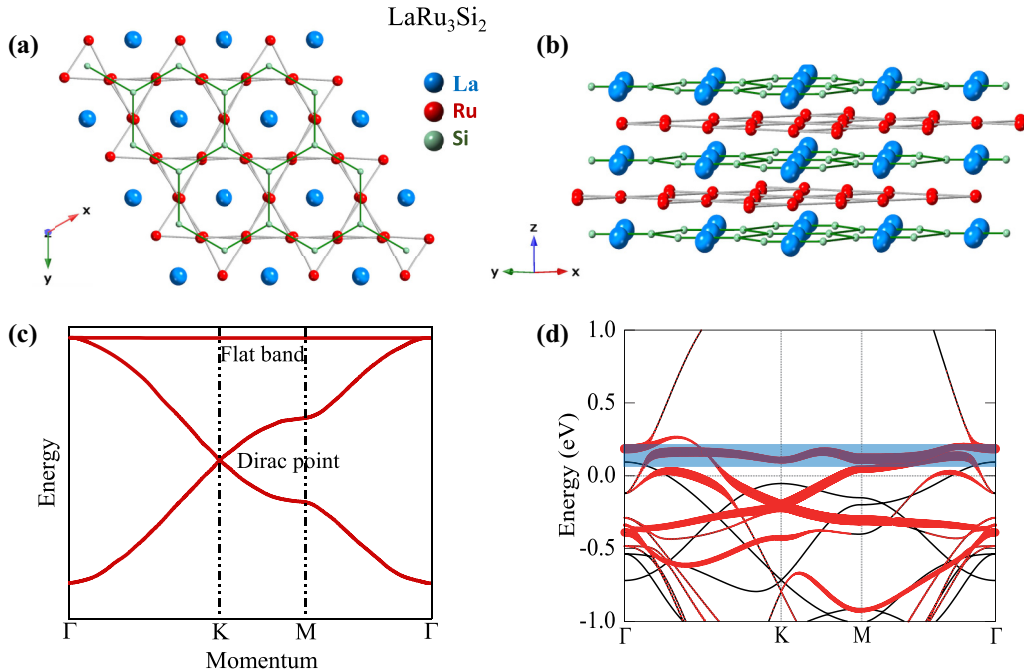


FIG. 1. Top view (a) and side view (b) of the atomic structure of LaRu<sub>3</sub>Si<sub>2</sub>. The Ru atoms construct a kagome lattice (red middle-size circles), while the Si (green small-size circles) and La atoms (blue large-size circles) form a honeycomb and triangular structure, respectively. (c) Tight-binding band structure of kagome lattice exhibiting two Dirac bands at the  $K$  point and a flat band across the whole Brillouin zone (BZ). (d) The band structures (black) and orbital-projected band structure (red) for the Ru- $d_{z^2}$  orbital without SOC along the high symmetry  $k$  path, presented in conformal kagome BZ. The width of the line indicates the weight of each component. The blue-colored region highlights the manifestation of the kagome flat band.

of LaRu<sub>3</sub>Si<sub>2</sub>. Thus, thorough and microscopic exploration of superconductivity in LaRu<sub>3</sub>Si<sub>2</sub> from both experimental and theoretical perspectives is required in order to understand the origin of the relatively high value of the critical temperature.

Here, we combine a powerful microscopic probe such as the muon spin rotation ( $\mu$ SR) [26–29] together with first-principles calculations [30–34] to elucidate the superconductivity in kagome superconductor LaRu<sub>3</sub>Si<sub>2</sub> with  $T_c \simeq 7$  K. We find that the calculated normal state band structure features a kagome flat band, and Dirac van Hove points formed by the Ru- $d_{z^2}$  orbitals near the Fermi level. The superfluid density obtained from  $\mu$ SR is best described by the scenario of a single SC gap function without nodes. The measured SC gap value  $\Delta = 1.14(1)$  meV yields a BCS ratio  $2\Delta/k_B T_c \simeq 4.3$ , suggesting that the superconductor LaRu<sub>3</sub>Si<sub>2</sub> is in the moderate coupling limit. We also find that the electron-phonon coupling alone turns out to be insufficient to reproduce the experimental critical temperature  $T_c$ , suggesting kagome lattice related factors in enhancing  $T_c$ .

## II. RESULTS AND DISCUSSIONS

The calculated total and projected density of state (DOS) (Fig. 2(a) and Fig. S4(a) of the Supplemental Material [35]) demonstrate that the states at the Fermi level in LaRu<sub>3</sub>Si<sub>2</sub> are mainly contributed by the Ru  $4d$  electrons. The band structure with the Ru- $d_{z^2}$  orbital projection is shown in Fig. 1(d). There are several bands that cross the Fermi level and the complex three-dimensional Fermi surfaces (Fig. 2(b) and Fig. S4(c) of the Supplemental Material [35]) are formed in the first Brillouin zone, indicating multiband physics. Most importantly,

in the  $k_z = 0$  plane, a flat band of the kagome lattice formed by the Ru- $d_{z^2}$  orbitals is found 0.1 eV above the Fermi level, highlighted by blue-colored region in Fig. 1(d). In addition, a Dirac point at the  $K$  ( $K'$ ) point with linear dispersion is found 0.2 eV below the Fermi level. Moreover, the van Hove point on the kagome lattice at the  $M$  point can be clearly seen in Fig. 1(d), which is located even closer to the Fermi energy ( $\sim 50$  meV). Thus, the system LaRu<sub>3</sub>Si<sub>2</sub> exhibits, around the Fermi level, a typical kagome lattice band structure [see Fig. 1(c)], revealing a Dirac point, the van Hove point, and a dispersionless, flat band that originates from the kinetic frustration associated with the geometry of the kagome lattice.

The temperature dependence of electrical resistivity for LaRu<sub>3</sub>Si<sub>2</sub>, depicted in Fig. 3(a) under different applied fields up to 9 T, shows superconductivity with the onset and the midpoint (at 50 % drop of the resistivity) of the transition at 7 K and 6.5 K, respectively. The upper critical magnetic field was estimated to be as high as  $\mu_0 H_{c2} = 8.5$  T at  $T = 2$  K (see Fig. S3 of the Supplemental Material [35]). In the following, we provide the microscopic details of the superconductivity in this system using  $\mu$ SR.

Figures 3(b) and 3(c) exhibit the transverse field (TF)  $\mu$ SR time spectra for LaRu<sub>3</sub>Si<sub>2</sub> in an applied magnetic field of 70 mT, measured at  $p = 0$  GPa and maximum applied pressure  $p = 1.85$  GPa, respectively. The spectra above (7 K) and below (0.25 K) the SC transition temperature  $T_c$  are shown. Above  $T_c$  the oscillations show a small damping due to the random local fields from the nuclear magnetic moments. Below  $T_c$  the damping rate strongly increases, with

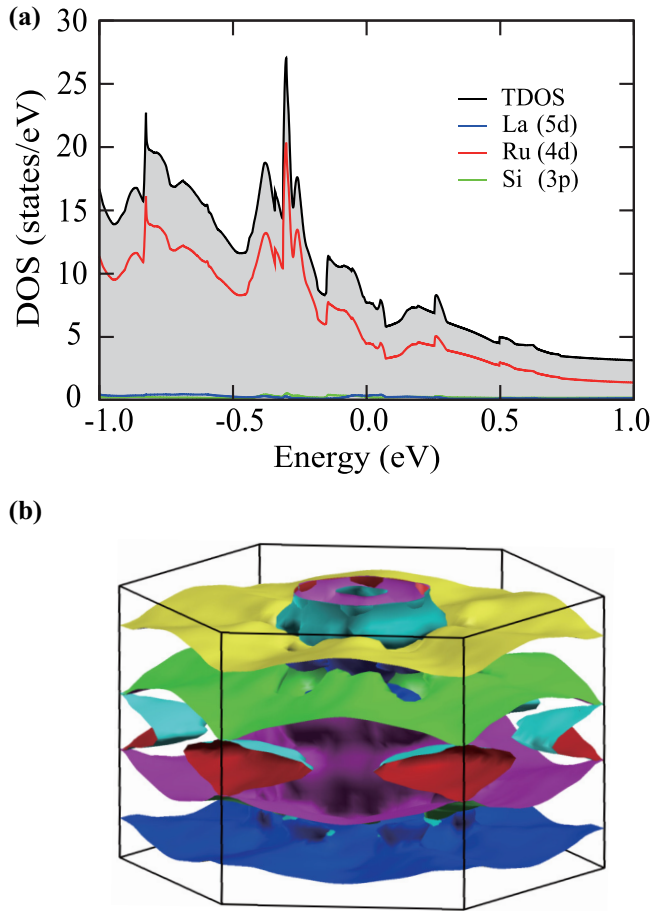


FIG. 2. (a) The calculated total DOS and projected DOS for the Ru, Si, and La atoms in the bulk  $\text{LaRu}_3\text{Si}_2$ . (b) Three-dimensional Fermi surface of  $\text{LaRu}_3\text{Si}_2$  in the first Brillouin zone.

decreasing temperature due to the presence of a nonuniform local magnetic field distribution as a result of the formation of a flux-line lattice (FLL) in the SC state. Magnetism, if present in the samples, may enhance the muon spin depolarization rate and falsify the interpretation of the TF- $\mu$ SR results. Therefore, we have carried out zero-field (ZF)- $\mu$ SR experiments above and below  $T_c$  to search for magnetism (static or weakly fluctuating) in  $\text{LaRu}_3\text{Si}_2$ . As shown in Fig. 3(d), no sign of either static or fluctuating magnetism could be detected in ZF time spectra down to 0.25 K. The spectra are well described by a Kubo-Toyabe depolarization function [36–38], reflecting the field distribution at the muon site created by the nuclear moments of the sample and the pressure cell. Returning to the discussion of the TF- $\mu$ SR data, we observe a strong diamagnetic shift of the internal magnetic field  $\mu_0 H_{\text{int}}$  sensed by the muons below  $T_c$ . This is evident in Fig. 3(e), where we plot the temperature dependence of  $\Delta\mu_0 H_{\text{int}} = \mu_0(H_{\text{int,SC}} - H_{\text{int,NS}})$ , i.e., the difference between the internal field  $\mu_0 H_{\text{int,SC}}$  measured in the SC fraction and  $\mu_0 H_{\text{int,NS}}$  measured in the normal state at  $T = 10$  K. The strong diamagnetic shift excludes the occurrence of field induced magnetism in  $\text{LaRu}_3\text{Si}_2$ . The absence of magnetism in ZF or under applied magnetic fields implies that the increase of the TF relaxation rate below  $T_c$  is solely arising from the FLL in the superconducting state.

From the TF- $\mu$ SR time spectra, we determined the Gaussian superconducting relaxation rate  $\sigma_{\text{sc}}$  (after subtracting the nuclear contribution), which is proportional to the second moment of the field distribution. Figure 2(f) shows  $\sigma_{\text{sc}}$  as a function of temperature for  $\text{LaRu}_3\text{Si}_2$  at  $\mu_0 H = 0.07$  T, recorded for various hydrostatic pressures. Below  $T_c$  the relaxation rate  $\sigma_{\text{sc}}$  starts to increase from zero due to the formation of the FLL. We note that both  $\sigma_{\text{sc}}$  and  $T_c$  stay nearly unchanged under pressure, indicating a robust superconducting state of  $\text{LaRu}_3\text{Si}_2$ . At all pressures,  $\sigma_{\text{sc}}(T)$  shows saturation towards low temperatures.

In order to investigate the symmetry of the SC gap, we note that temperature dependence of the magnetic penetration depth  $\lambda(T)$  is related to the relaxation rate  $\sigma_{\text{sc}}(T)$  in the presence of a perfect triangular vortex lattice by the equation [27]:

$$\frac{\sigma_{\text{sc}}(T)}{\gamma_{\mu}} = 0.06091 \frac{\Phi_0}{\lambda_{\text{eff}}^2(T)}, \quad (1)$$

where  $\gamma_{\mu}$  is the gyromagnetic ratio of the muon and  $\Phi_0$  is the magnetic-flux quantum. Thus, the flat  $T$ -dependence of  $\sigma_{\text{sc}}$  observed at various pressures for low temperatures [see Fig. 3(f)] is consistent with a nodeless superconductor, in which  $\lambda_{\text{eff}}^{-2}(T)$  reaches its zero-temperature value exponentially. We note that it is the effective penetration depth  $\lambda_{\text{eff}}^{-2}$  (powder average), which we extract from the  $\mu$ SR depolarization rate (Eq. 1), and this is the one shown in the figures. The magnetic penetration depth is one of the fundamental parameters of a superconductor, since it is related to the superfluid density  $n_{\text{sc}}$  via  $1/\lambda_{\text{eff}}^2 = \mu_0 e^2 n_{\text{sc}}/m^*$  (where  $m^*$  is the effective mass and  $n_s$  is the SC carrier density). A quantitative analysis of  $\lambda_{\text{eff}}(T)$  [26,39–41] is described in the methods section of the supplementary information. The results of this analysis are presented in Figs. 4(a)–4(c), where the temperature dependence of  $\lambda_{\text{eff}}^{-2}$  for  $\text{LaRu}_3\text{Si}_2$  is plotted at various pressures. The solid and dashed lines represent fits to the data using  $s$ -wave and  $d$ -wave models, respectively. As seen in Fig. 4,  $\lambda_{\text{eff}}(T)$  dependence is best described by a momentum independent  $s$ -wave model with a gap value of  $\Delta = 1.2(1)$  meV and  $T_c \simeq 6.5$  K. The effective penetration depth,  $\lambda_{\text{eff}}$ , at zero temperature is found to be 240(10) nm. We also tested the power law  $[1-(T/T_c)^2]$  which has been proposed theoretically [42] for the superfluid density of dirty  $d$ -wave superconductors and found it to be inconsistent with the data. The observed single gap superconductivity in this multiband system implies that the superconducting pairing involves predominately one band. However, if the interband coupling is strong, then one may detect single-gap-like behavior of the superfluid density even in multigap materials [43].

The ratio of the superconducting gap to  $T_c$  for  $\text{LaRu}_3\text{Si}_2$  was estimated to be  $(2\Delta/k_B T_c) \simeq 4.3$ , which is large. However it is not out of the limit of conventional superconductivity, since similar values for  $2\Delta/k_B T_c$  were found for conventional superconductors such as Pb and Hg [44]. On the other hand, a similar ratio can also be expected for Bose Einstein Condensate (BEC)-like picture as pointed out in references [45,49]. To place this system  $\text{LaRu}_3\text{Si}_2$  in the context of other superconductors, in Fig. 4(d) we plot the critical temperature  $T_c$  against the superfluid density  $\lambda_{\text{eff}}^{-2}$ . Most unconventional

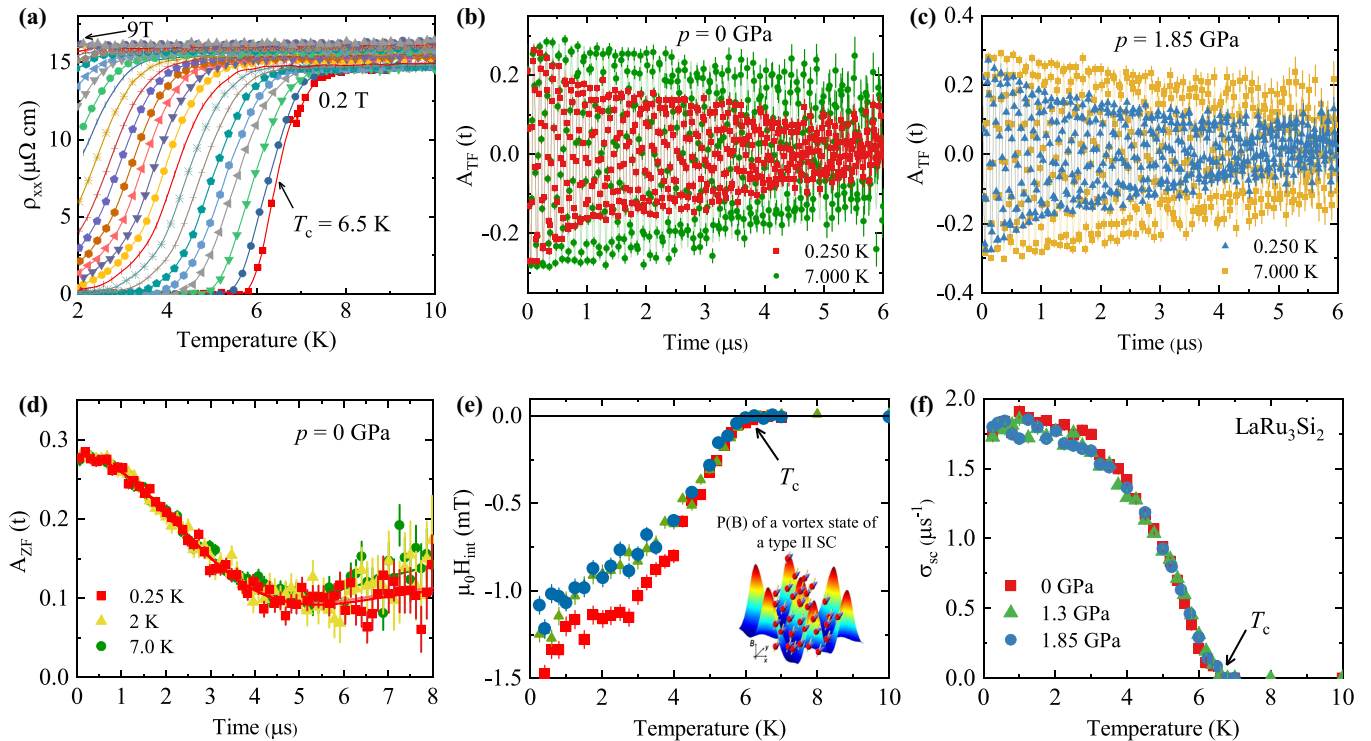


FIG. 3. (a) The temperature dependence of the electrical resistivity for  $\text{LaRu}_3\text{Si}_2$ , recorded for various applied magnetic fields. (b–d) Transverse-field (TF) and zero-field (ZF)  $\mu\text{SR}$  time spectra for  $\text{LaRu}_3\text{Si}_2$  to probe the SC vortex state and magnetic responses, respectively. The TF spectra are obtained above and below  $T_c$  (after field cooling the sample from above  $T_c$ ): (b)  $p = 0$  GPa and (c)  $p = 1.85$  GPa. The solid lines in (b) and (c) represent fits to the data by means of Eq. (1) of the supplementary information. Inset illustrates how muons, as local probes, sense the inhomogeneous field distribution in the vortex state of the type-II superconductor. (d) ZF  $\mu\text{SR}$  time spectra for  $\text{LaRu}_3\text{Si}_2$  recorded above and below  $T_c$ . The line represents the fit to the data using a standard Kubo-Toyabe depolarization function [36], reflecting the field distribution at the muon site created by the nuclear moments. Temperature dependence of the diamagnetic shift  $\Delta\mu_0 H_{\text{int}}$  (e) and the muon spin depolarization rate  $\sigma_{\text{sc}}(T)$  (f), measured at various hydrostatic pressures in an applied magnetic field of  $\mu_0 H = 70$  mT. The arrows mark the  $T_c$  values.

superconductors have  $T_c/\lambda_{\text{eff}}^{-2}$  values of about 0.1–20, whereas all of the conventional BCS superconductors lie on the far right in the plot, with much smaller ratios. In the other words, unconventional superconductors are characterized by a dilute superfluid (low density of Cooper pairs), while conventional BCS superconductors exhibit dense superfluids. Moreover, a linear relationship between  $T_c$  and  $\lambda_{\text{eff}}^{-2}$  is expected only on the Bose Einstein Condensate (BEC)-like side and is considered a hallmark feature of unconventional superconductivity. We recently showed that the linear correlation is an intrinsic property of the superconductivity in transition metal dichalcogenides [45,46], whereas the ratio  $T_c/\lambda_{\text{eff}}^{-2}$  is lower than the ratio observed in hole-doped cuprates [see Figure 4(d)]. For twisted bilayer graphene [18] the ratio  $T_c/\lambda_{\text{eff}}^{-2}$  was found to be even higher than the one for cuprates. For  $\text{LaRu}_3\text{Si}_2$  the ratio is estimated to be  $T_c/\lambda_{\text{eff}}^{-2} \simeq 0.37$ , which is approximately a factor of 15 lower than the one for hole-doped cuprates, but still is far away from conventional phonon-mediated BCS superconductors. Interestingly, the point for  $\text{LaRu}_3\text{Si}_2$  is almost perfectly located on the trend line on which charge density wave superconductors  $2\text{H-NbSe}_2$  and  $4\text{H-NbSe}_2$ , as well as Weyl-superconductor  $T_d\text{-MoTe}_2$  [45], lie, as shown in Fig. 4(d). This finding hints, to some extent, at a mechanism beyond BCS pairing responsible for superconductivity in  $\text{LaRu}_3\text{Si}_2$ . Such a mechanism has a low density of Cooper

pairs and similar electron correlations as in  $2\text{H-NbSe}_2$  and  $T_d\text{-MoTe}_2$ , but much weaker electron correlations than in cuprates and twisted bilayer graphene.

Since the present muon spin rotation experiments show direct evidence for the absence of local moments of the Ru atom in  $\text{LaRu}_3\text{Si}_2$ , this kagome system is different from high- $T_c$  superconductors or spin liquid compounds. It is rather on the side of itinerant kagome or hexagonal systems such as  $(\text{Cs},\text{K})\text{V}_3\text{Sb}_5$  [53] or even  $2\text{H-NbSe}_2$  [46], where  $\mu\text{SR}$  shows the absence of magnetic correlations. On the other hand, the system  $\text{LaRu}_3\text{Si}_2$  does not exhibit a CDW ground state unlike the superconductors  $(\text{Cs},\text{K})\text{V}_3\text{Sb}_5$  [54]. One possibility is that this system is just somewhat away from CDW order and has higher optimal  $T_c$ . The fact that the stability of the crystal structure is obtained with the addition of the Hubbard  $U$  (see the Supplemental Material [35]) suggests proximity of this superconductor  $\text{LaRu}_3\text{Si}_2$  to a CDW, since  $U$  opposes the CDW. Pressure independent superfluid density was recently reported for CDW free layered transition metal dichalcogenide system  $2\text{M-WS}_2$  [55], while a large enhancement of  $\lambda_{\text{eff}}^{-2}$  was found in CDW superconductor  $2\text{H-NbSe}_2$  under pressure when suppressing the CDW order [46]. Thus, the robustness of both  $T_c$  and the superfluid density  $\lambda_{\text{eff}}^{-2}$  of  $\text{LaRu}_3\text{Si}_2$  to hydrostatic pressure strongly suggests that  $T_c$  has the optimal value already at ambient pressure,

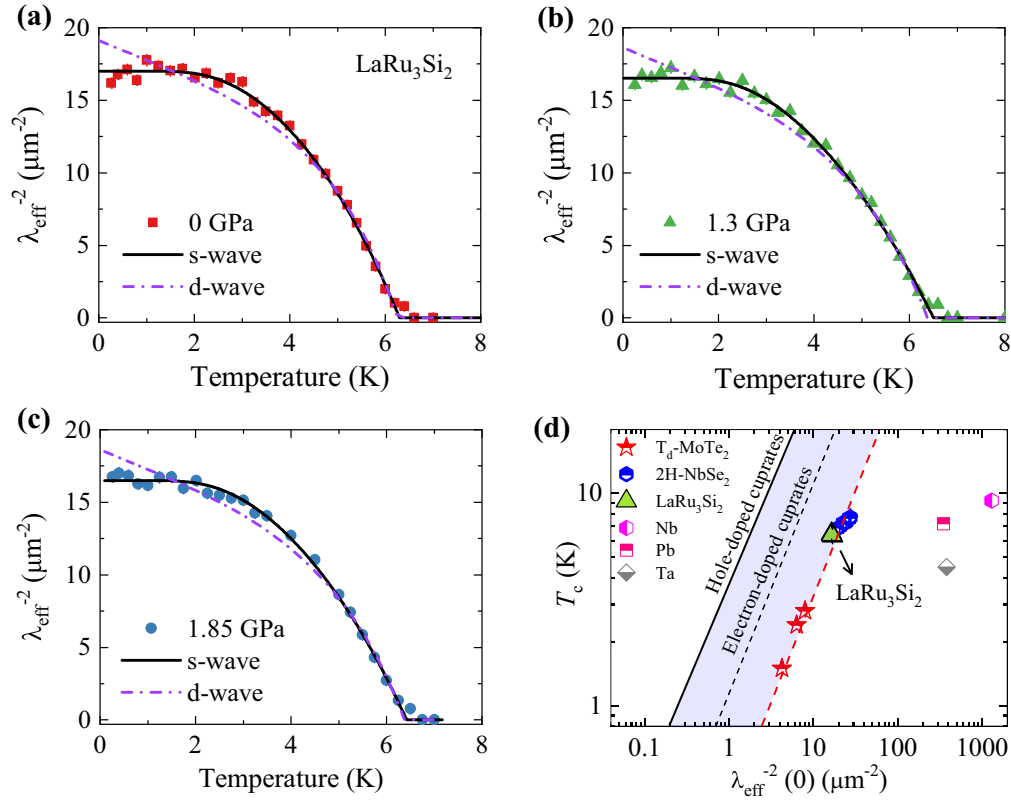


FIG. 4. The temperature dependence of  $\lambda_{\text{eff}}^{-2}$  measured at various applied hydrostatic pressures for  $\text{LaRu}_3\text{Si}_2$ : (a)  $p = 0$  GPa, (b) 1.3 GPa, and (c) 1.85 GPa. The solid line corresponds to an  $s$ -wave model and the dashed line represents fitting with a  $d$ -wave model. (d) A plot of  $T_c$  versus the  $\lambda_{\text{eff}}^{-2}(0)$  obtained from our  $\mu\text{SR}$  experiments in  $\text{LaRu}_3\text{Si}_2$ . The dashed red line represents the relation obtained for layered transition metal dichalcogenide superconductors  $T_d$ - $\text{MoTe}_2$  [45] and  $2\text{H-NbSe}_2$  [46]. The data are taken at ambient conditions as well as under pressure. The relation observed for underdoped cuprates is also shown (solid line for hole doping [47–50] and the dashed black line for electron doping [51,52]). The points for various conventional BCS superconductors are also shown.

and that the system is away from a competing CDW ground state.

In order to understand the origin of  $T_c$ , we compare experimentally measured critical temperatures with those calculated using the McMillan equation [56,57]. The phonon dispersion for  $\text{LaRu}_3\text{Si}_2$ , calculated by the GGA + U method with  $U = 1$  eV is shown in Fig. S4(d) in the Supplemental Material [35]. It consists of only the positive frequency modes, and the optimized lattice constants agree very well with the experimental parameters. Based on the phonon dispersion, we calculated the electron-phonon coupling constant  $\lambda_{e,\text{ph}}$  to be  $\simeq 0.45$ , indicating only a moderate coupling strength in  $\text{LaRu}_3\text{Si}_2$ . For such a low value of  $\lambda_{e,\text{ph}}$ , the following McMillan equation gives a precise estimate of the electron-phonon interaction induced critical temperature, as discussed in Ref. [57]:

$$T_c = \frac{\theta}{1.45} \exp \left[ -\frac{1.04(1 + \lambda_{e,\text{ph}})}{\lambda_{e,\text{ph}} - \mu^*(1 + 0.62\lambda_{e,\text{ph}})} \right] \quad (2)$$

By using  $\lambda_{e,\text{ph}} \simeq 0.45$ , Debye temperature  $\theta = 280$  K, and the Coulomb pseudo potential  $\mu^* = 0.12$ , the superconducting transition temperature  $T_c$  was estimated to be  $T_c \simeq 1.2$  K. The calculated value of  $T_c$  is obviously much smaller than

the experimental value. Since the electron-phonon coupling can reproduce only a small fraction of the experimental  $T_c$ , other factors in enhancing  $T_c$  must be considered. The calculations show the presence of a flat band near the Fermi level, which may enhance correlations and can contribute to the enhancement of  $T_c$  in this system. However, the flat band is 100 meV above  $E_f$  and it may not have a key role in enhancing  $T_c$ . The van Hove point on the kagome lattice at M point, seen in Fig. 1(d), is located even closer to the Fermi energy ( $\sim 50$  meV), which can also contribute to the enhancement of  $T_c$ . This van Hove point at M is of a similar distance to  $E_f$  (below  $E_f$ ) in  $\text{KV}_3\text{Sb}_5$ , and is what was shown to drive the  $2 \times 2$  CDW order [54] at much higher temperatures than  $T_c$ . Moreover, we find that the whole kagome bands are somewhat narrow ( $\sim 300$  meV), which may also enhance  $T_c$  through the overall higher density of states. The narrowness of the kagome bands to be  $\sim 300$  meV may be formally similar to a group of narrow bands found in twisted bilayer graphene [18].

### III. SUMMARY

We provide a microscopic investigation of superconductivity in the layered distorted kagome superconductor  $\text{LaRu}_3\text{Si}_2$  with a bulk probe. Specifically, the zero-temperature magnetic

penetration depth  $\lambda_{\text{eff}}(0)$  and the temperature dependence of  $\lambda_{\text{eff}}^{-2}$  were studied by means of  $\mu$ SR experiments. The superfluid density is best described by the scenario of a gap function without nodes. Interestingly, the  $T_c/\lambda_{\text{eff}}^{-2}$  ratio is far away from those of conventional phonon-mediated BCS superconductors, suggesting that to some extent superconductivity in  $\text{LaRu}_3\text{Si}_2$  is mediated by some pairing mechanism beyond BCS pairing, evidenced by the low density of Cooper pairs. Furthermore, we find the calculated normal state band structure features a kagome flat band, Dirac point, and van Hove point formed by the  $\text{Ru-}dz^2$  orbitals near the Fermi level. The electron-phonon coupling induced critical temperature  $T_c$ , estimated from the phonon dispersion, was found to be much smaller than the experimental value. Thus, the enhancement of  $T_c$  in  $\text{LaRu}_3\text{Si}_2$  is attributed to the presence of the flat band and the van Hove point relatively close to the Fermi level, as well as to the high density of states from the narrow kagome bands. Our experiments and calculations taken together point to nodeless kagome superconductivity in  $\text{LaRu}_3\text{Si}_2$ .

### ACKNOWLEDGMENTS

$\mu$ SR experiments under pressure were performed at the  $\mu$ E1 beamline of the Paul Scherrer Institute (Villigen,

Switzerland) using the instrument GPD, where an intense high-energy ( $p_\mu = 100$  MeV/c) beam of muons is implanted in the sample through the pressure cell. Further details of sample characterization and calculations may be found in the Supplemental Material [35]. Z.G. thanks Rafael Fernandes for useful discussions. M.Z.H. acknowledges visiting scientist support from IQIM at the California Institute of Technology. Z.Q.W. is supported by DOE grant No. DE-FG02-99ER45747. G.X. and Y.Q. would like to thank the support of the National Key Research and Development Program of China (2018YFA0307000) and the National Natural Science Foundation of China (11874022). Work at Princeton University was supported by the Gordon and Betty Moore Foundation (GBMF4547 and GBMF9461; M.Z.H.). The theoretical work and sample characterization are supported by the United States Department of Energy (U.S. DOE) under the Basic Energy Sciences programme (Grant No. DOE/BES DE-FG-02-05ER46200; M.Z.H.). This work was also supported by the National Natural Science Foundation of China Grants No. 11774007 and No. U1832214, the National Key R&D Program of China (2018YFA0305601) and the strategic Priority Research Program of Chinese Academy of Sciences, Grant No. XDB28000000.

- 
- [1] J.-X. Yin *et al.*, *Nature (London)* **562**, 91 (2018).  
 [2] L. Ye *et al.*, *Nature (London)* **555**, 638 (2018).  
 [3] T.-H. Han *et al.*, *Nature (London)* **492**, 406 (2012).  
 [4] J.-X. Yin, S. S. Zhang, G. Chang, Q. Wang, S. Tsirkin, Z. Guguchia, B. Lian, H. Zhou, K. Jiang, I. Belopolski, N. Shumiya, D. Multer, M. Litskevich, T. A. Cochran, H. Lin, Z. Wang, T. Neupert, S. Jia, H. Lei, M. Z. Hasan, *Nat. Phys.* **15**, 443 (2019).  
 [5] Z. Guguchia, J. Verezhak, D. Gawryluk, S. S. Tsirkin, J.-X. Yin, I. Belopolski, H. Zhou, G. Simutis, S.-S. Zhang, T. A. Cochran, G. Chang, E. Pomjakushina, L. Keller, Z. Skrzeczowska, Q. Wang, H. C. Lei, R. Khasanov, A. Amato, S. Jia, T. Neupert, H. Luetkens, M. Z. Hasan, *Nat. Commun.* **11**, 559 (2020).  
 [6] O. V. Yazyev, *Nat. Phys.* **15**, 424 (2019).  
 [7] N. J. Ghimire and I. I. Mazin, *Nat. Mater.* **19**, 137 (2020).  
 [8] J. S. Hofmann, E. Berg, and D. Chowdhury, *Phys. Rev. B* **102**, 201112(R) (2020).  
 [9] L. H. C. M. Nunes and C. M. Smith, *Phys. Rev. B* **101**, 224514 (2020).  
 [10] G. E. Volovik, *JETP Lett.* **107**, 516 (2018).  
 [11] T. T. Heikkila, N. B. Kopnin, and G. E. Volovik, *JETP Lett.* **94**, 233 (2011).  
 [12] N. B. Kopnin, T. T. Heikkila, and G. E. Volovik, *Phys. Rev. B* **83**, 220503(R) (2011).  
 [13] E. H. Lieb, *Phys. Rev. Lett.* **62**, 1201 (1989).  
 [14] A. Tanaka and H. Ueda, *Phys. Rev. Lett.* **90**, 067204 (2003).  
 [15] K. Noda, A. Koga, N. Kawakami, and T. Pruschke, *Phys. Rev. A* **80**, 063622 (2009).  
 [16] A. Julku, S. Peotta, T. I. Vanhala, D.-H. Kim, and P. Torma, *Phys. Rev. Lett.* **117**, 045303 (2016).  
 [17] N. Hartman, W.-T. Chiu, and R. T. Scalettar, *Phys. Rev. B* **93**, 235143 (2016).  
 [18] Y. Cao, V. Fatemi, A. Demir, S. Fang, S. L. Tomarken, J. Y. Luo, J. D. Sanchez-Yamagishi, K. Watanabe, T. Taniguchi, E. Kaxiras, R. C. Ashoori, and P. Jarillo-Herrero, *Nature (London)* **556**, 80 (2018).  
 [19] S. Peotta and P. Torma, *Nat. Commun.* **6**, 8944 (2015).  
 [20] S. Sayyad, E. W. Huang, M. Kitatani, M.-S. Vaezi, Z. Nussinov, A. Vaezi, and H. Aoki, *Phys. Rev. B* **101**, 014501 (2020).  
 [21] H. Barz, *Mater. Res. Bull. PNAS* **15**, 1489 (1980).  
 [22] J. M. Vandenberg and H. Barz, *Materials Research Bulletin* **15**, 1493 (1980).  
 [23] Y. Kishimoto, T. Ohno, T. Hihara, K. Sumiyama, G. Ghosh, and L. C. Gupta, *J. Phys. Soc. Jpn.* **71**, 2035 (2002).  
 [24] B. Li, S. Li, and H.-H. Wen, *Phys. Rev. B* **94**, 094523 (2016).  
 [25] S. Li, B. Zeng, X. Wan, F. Han, J. Tao, H. Yang, Z. Wang, and H.-H. Wen, Anomalous Properties in the Normal and Superconducting States of  $\text{LaRu}_3\text{Si}_2$ , *Phys. Rev. B* **84**, 214527 (2011).  
 [26] J. E. Sonier, J. H. Brewer, and R. F. Kiefl, *Rev. Mod. Phys.* **72**, 769 (2000).  
 [27] E. H. Brandt, *Phys. Rev. B* **37**, 2349 (1988).  
 [28] Z. Guguchia, A. Amato, J. Kang, H. Luetkens, P. K. Biswas, G. Prando, F. von Rohr, Z. Bukowski, A. Shengelaya, H. Keller, E. Morenzoni, R. M. Fernandes, and R. Khasanov, Direct evidence for the emergence of a pressure induced nodal superconducting gap in the iron-based superconductor  $\text{Ba}_{0.65}\text{Rb}_{0.35}\text{Fe}_2\text{As}_2$ , *Nat. Commun.* **6**, 8863 (2015).  
 [29] G. M. Luke, Y. Fudamoto, K. M. Kojima, M. I. Larkin, J. Merrin, B. Nachumi, Y. J. Uemura, Y. Maeno, Z. Q. Mao, Y. Mori, H. Nakamura, and M. Sigrist, *Nature (London)* **394**, 558 (1998).  
 [30] G. Kresse and J. Furthmüller, *Phys. Rev. B* **54**, 11169 (1996).  
 [31] J. P. Perdew, K. Burke, and M. Ernzerhof, *Phys. Rev. Lett.* **77**, 3865 (1996).

- [32] V. I. Anisimov, J. Zaanen, and O. K. Andersen, *Phys. Rev. B* **44**, 943 (1991).
- [33] P. Giannozzi, S. De Gironcoli, P. Pavone, and S. Baroni, *Phys. Rev. B* **43**, 7231 (1991).
- [34] A. Togo, Phonopy, <https://atztogo.github.io/phonopy>.
- [35] See Supplemental Material at <http://link.aps.org/supplemental/10.1103/PhysRevMaterials.5.034803> for the details of sample characterization and calculations.
- [36] R. Kubo and T. Toyabe, *Magnetic Resonance and Relaxation* (North Holland, Amsterdam, 1967).
- [37] R. Khasanov, Z. Guguchia, A. Maisuradze, D. Andreica, M. Elender, A. Raselli, Z. Shermadini, T. Goko, F. Knecht, E. Morenzoni, and A. Amato, *High Press. Res.* **36**, 140 (2016).
- [38] Z. Shermadini, R. Khasanov, M. Elender, G. Simutis, Z. Guguchia, K. V. Kamenev, and A. Amato, *High Press. Res.* **37**, 449 (2017).
- [39] A. Suter and B. M. Wojek, *Phys. Procedia* **30**, 69 (2012). The fitting of the  $T$ -dependence of the penetration depth with  $\alpha$  model was performed using the additional library BMW developed by B. M. Wojek.
- [40] M. Tinkham, *Introduction to Superconductivity* (Krieger Publishing Company, Malabar, Florida, 1975).
- [41] A. Carrington, and F. Manzano, *Physica C* **385**, 205 (2003).
- [42] P. J. Hirschfeld, W. O. Putikka, and D. J. Scalapino, *Phys. Rev. B* **50**, 10250 (1994).
- [43] R. Gupta, C. Lohnert, C. Wang, D. Johrendt, H. Luetkens, S. Malick, T. Shiroka, Z. Hossain, and R. Khasanov, *Phys. Rev. B* **102**, 144515 (2020).
- [44] G. W. Webb, F. Marsiglio, and J. E. Hirsch, *Physica C* **514**, 17 (2015).
- [45] Z. Guguchia, F. von Rohr, Z. Shermadini, A. T. Lee, S. Banerjee, A. R. Wieteska, C. A. Marianetti, B. A. Frandsen, H. Luetkens, Z. Gong, S. C. Cheung, C. Baines, A. Shengelaya, G. Taniashvili, A. N. Pasupathy, E. Morenzoni, S. J. L. Billinge, A. Amato, R. J. Cava, R. Khasanov, Y. J. Uemura, *Nat. Commun.* **8**, 1082 (2017).
- [46] F. O. von Rohr, J.-C. Orain, R. Khasanov, C. Witteveen, Z. Shermadini, A. Nikitin, J. Chang, A. R. Wieteska, A. N. Pasupathy, M. Z. Hasan, A. Amato, H. Luetkens, Y. J. Uemura, Z. Guguchia, *Sci. Adv.* **5**, eaav8465 (2019).
- [47] Y. J. Uemura, G. M. Luke, B. J. Sternlieb, J. H. Brewer, J. F. Carolan, W. N. Hardy, R. Kadono, J. R. Kempton, R. F. Kiefl, S. R. Kreitzman, P. Mulhern, T.M. Riseman, D. L. Williams, B. X. Yang, S. Uchida, H. Takagi, J. Gopalakrishnan, A. W. Sleight, M. A. Subramanian, C.L. Chien, M. Z. Cieplak, G. Xiao, V. Y. Lee, B. W. Statt, C. E. Stronach, W. J. Kossler, and X. H. Yu, *Phys. Rev. Lett.* **62**, 2317 (1989).
- [48] Y. J. Uemura *et al.*, *Nature (London)* **352**, 605 (1991).
- [49] Y. J. Uemura *et al.*, *Phys. Rev. Lett.* **66**, 2665 (1991).
- [50] Y. J. Uemura, *J. Phys.: Condens. Matter* **16**, S4515 (2004).
- [51] H. Luetkens, H.-H. Klauss, M. Kraken, F. J. Litterst, T. Dellmann, R. Klingeler, C. Hess, R. Khasanov, A. Amato, C. Baines, M. Kosmala, O. J. Schumann, M. Braden, J. Hamann-Borrero, N. Leps, A. Kondrat, G. Behr, J. Werner, and B. Büchner, *Nat. Mater.* **8**, 305 (2009).
- [52] A. Shengelaya, R. Khasanov, D. G. Eshchenko, D. Di Castro, I. M. Savic, M. S. Park, K. H. Kim, S. I. Lee, K. A. Müller, and H. Keller, *Phys. Rev. Lett.* **94**, 127001 (2005).
- [53] E. M. Kenney, B. R. Ortiz, C. Wang, S. D. Wilson, and M. J. Graf, Absence of local moments in the kagome metal  $KV_3Sb_5$  as determined by muon spin spectroscopy, *J. Phys.: Condens. Matter* (2021), doi: 10.1088/1361-648X/abe8f9.
- [54] Y.-X. Jiang, J.-X. Yin, M. Denner, N. Shumiya, B. R. Ortiz, J. He, X. Liu, S. S. Zhang, G. Chang, I. Belopolski, Q. Zhang, S. Hossain, T. A. Cochran, D. Multer, M. Litskevich, Z.-J. Cheng, X. P. Yang, Z. Guguchia, G. Xu, Z. Wang, T. Neupert, S. D. Wilson, and M. Z. Hasan, Discovery of topological charge density wave in kagome superconductor  $KV_3Sb_5$ , [arXiv:2012.15709](https://arxiv.org/abs/2012.15709).
- [55] Z. Guguchia, D. J. Gawryluk, M. Brzezinska, S. S. Tsirkin, R. Khasanov, E. Pomjakushina, F. O. von Rohr, J. A. T. Verezhak, M. Z. Hasan, T. Neupert, H. Luetkens, and A. Amato, *npj Quantum Mater.* **4**, 50 (2019).
- [56] W. L. McMillan, *Phys. Rev.* **167**, 331 (1968).
- [57] J. P. Carbotte, *Rev. Mod. Phys.* **62**, 1027 (1990).